Eur Radiol (2006) 16: 161–165
DOI 10.1007/s00330-005-2813-y

EXPERIMENTAL

Etienne Ketelslegers
Bernard E. Van Beers

Urinary calculi: improved detection and characterization with thin-slice multidetector CT

Received: 19 October 2004
Revised: 5 April 2005
Accepted: 29 April 2005
Published online: 16 June 2005

E. Ketelslegers · B. E. Van Beers (✉)
Diagnostic Radiology Unit,
Cliniques Universitaires St-Luc,
Université Catholique de Louvain,
Avenue Hippocrate 10,
1200 Brussels, Belgium
e-mail: vanbeers@rdgn.ucl.ac.be
Tel.: +32-2-7642945
Fax: +32-2-7705574

Abstract The aim of this study was to assess the effect of reconstructed slice thickness on the detection and characterization of human urinary calculi on a multidetector helical CT scanner. Nineteen human urinary calculi of various chemical composition measuring 1.0–3.7 mm were embedded into agar in a chamber of a nylon body phantom. The phantom was imaged with a four detector-row CT scanner. The number of detected calculi increased as the reconstructed slice thickness decreased. Measured diameters and density of the visible calculi decreased as the slice thickness increased. The results of the present study support the use of thin reconstructed slices to detect and characterize urinary calculi.

Keywords Computed tomography · Reconstructed slice thickness · Kidney · Calculi · Ureter

Introduction

Computed tomography (CT) has become the preferred diagnostic method for the detection of urinary calculi [1–3]. This method can reveal calculi more accurately than standard radiography [4–6], sonography [7], and excretory urography [8]. Furthermore, the clinical outcome of renal colic may be predicted by accurate determination of the stone diameter [9, 10] and density measurements have been suggested as a possible aid in the prediction of the composition of urolithiasis [11–13]. Finally, alternative urinary or extra-urinary causes of acute flank pain can be detected by helical CT [2, 14]. These advantages allow increased diagnostic confidence and therapeutic efficacy in patients with suspected renal colic.

However, experimental and clinical studies have shown that some urinary calculi may be missed at helical CT [15, 16]. A false-negative rate of up to 7% has been reported and has been attributed to a combination of volume averaging (small stone size relative to slice thickness) and stone composition [16]. Despite the introduction of multidetector CT scanners, few attempts have been made in the literature to modify the CT acquisition parameters for the detection of urinary calculi since the description of the method by Smith et al. in 1995 [6, 15–19]. In particular, the effect of decreasing the reconstructed slice thickness has not been explored systematically and the use of 5-mm-thick slices is still being recommended for multidetector CT scanners [20].

The aim of this study was to assess the effect of slice thickness on the detection and characterization of human urinary calculi in a body phantom by means of a multidetector CT scanner.

Materials and methods

Nineteen human urinary calculi were obtained from consecutive patients who underwent nephrolithotomy or had spontaneous stone passage. The calculi were analyzed by microscopic inspection, chemical reaction, and, when appropriate, infrared spectroscopy. According to the main stone constituent, the calculi were divided into the five following groups: uric acid (n=4), cystine (n=3), calcium hydrogen phosphate dihydrate (n=4), magnesium ammonium phosphate hexahydrate (n=4), and calcium oxalate

(n=4). The calculi had diameters ranging from 1.0 to 3.7 mm, as measured before implantation into the body phantom. The calculi were individually embedded into 18 g/l agar gel in a 30-mm-diameter chamber of a 300-mm-diameter nylon cylinder (Fig. 1). The calculi were regularly spaced in three distinct transverse layers according to their size: 1.0–1.9 mm (n=9), 2.0–2.9 mm (n=5), and 3.0–3.7 mm (n=5). The layer of 1.0–1.9 mm contained two calculi composed of uric acid, one of cystine, two of calcium hydrogen phosphate dihydrate, two of magnesium ammonium phosphate hexahydrate, and two of calcium oxalate. The layer of 2–2.9 mm contained one calculus of each composition, as did the layer of 3–3.7 mm (Table 1).

CT scanning was performed with a four detector-row CT scanner (Mx8000 Quad, Philips Medical Systems, Best, The Netherlands). All scans were obtained during the same session with a peak kilovoltage of 120 kVp, a field-of-view of 400 mm, and a matrix size of 512×512. A reference scan was first obtained with a slice thickness of 0.5 mm and 1,000 mAs (Fig. 1). This scan was acquired to verify the positioning of the calculi in the transverse plane. The next scans were obtained with an effective current-time product of 140 mAs and a pitch of 1.75. Helical pitch was defined as the ratio of table movement per 360° rotation divided by the total collimated X-ray width [21]. Effective current-time product was defined as the product of the tube current intensity and the gantry rotation time, divided by the pitch [22]. The following slice thicknesses were used for reconstruction: 0.5, 1.0, 2.5, 5.0, and 10.0 mm. All images were reconstructed with a standard algorithm.

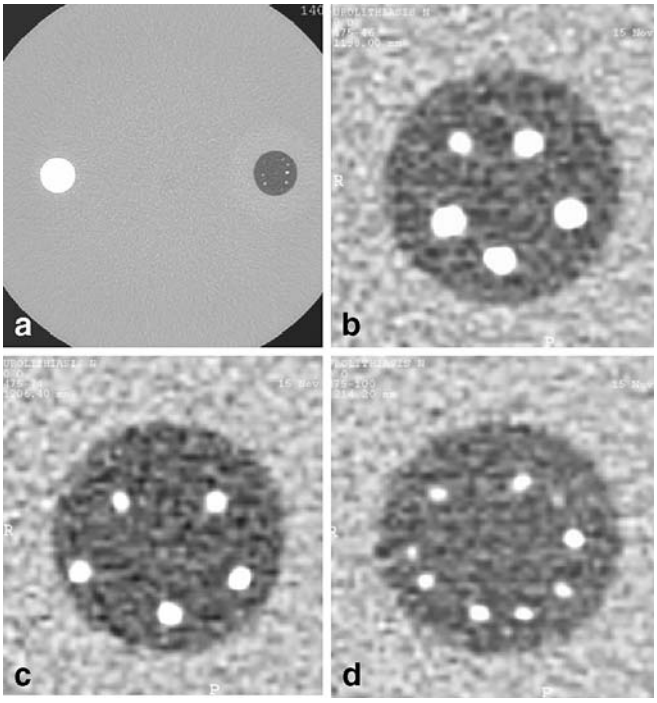

Fig. 1 **a** Transverse CT scan of the 300-mm-diameter body phantom. **b**–**d** Magnified reference CT scans of the 30-mm-diameter chamber of the phantom obtained at 1,000 mAs with a slice thickness of 0.5 mm. The calculi were regularly spaced in three distinct transverse layers according to their size: 1.0–1.9 mm (**b**), 2.0–2.9 mm (**c**), and 3.0–3.7 mm (**d**)

Table 1 Composition of urinary calculi according to their size

Composition	1–1.9 mm	2–2.9 mm	3–3.7 mm
Uric acid	2	1	1
Cystine	1	1	1
Calcium hydrogen phosphate dihydrate	2	1	1
Magnesium ammonium phosphate hexahydrate	2	1	1
Calcium oxalate	2	1	1

The CT series were visualized on a clinical workstation (MxView, Philips Medical Systems) with soft-tissue windows identical to those used in our clinical practice (width=360 H, center=60 H). Two investigators independently recorded the number of calculi identified on each series by using a scale from 0 to 2 (0=stone not detectable, 1=stone possibly present, 2=stone definitively present). All calculi with discordant scores were re-evaluated, with differences being resolved by consensus. An investigator measured the transverse diameter and density of the calculi detected at each slice thickness by using electronic calipers and manual delineation, respectively. For density measurements, a region of interest was created overlying the whole calculus on the slice in which it was seen at its largest diameter [13]. The mean value with standard deviation of transverse diameter and density of the visible calculi were calculated for each slice thickness. Image noise was measured as the standard deviation of the density in a 50-mm^2 region-of-interest in the center of the chamber.

Inter-observer agreement for the detection of calculi was calculated by using non-weighted binary kappa statistics. Spearman's correlation coefficient was calculated to determine the linearity of the data. The two-tailed Fisher's exact test was used to compare the proportion of calculi detected with each of the modalities. For this purpose, the calculi assigned a confidence level of 1 were considered not visible. A P value of less than 0.05 was considered statistically significant.

Results

The kappa coefficient for the two readers indicated excellent inter-observer agreement (κ=0.87). It was therefore statistically acceptable to consider the consensus reading to analyze the results. The number of calculi visualized at each slice thickness is shown in Fig. 2. More calculi were

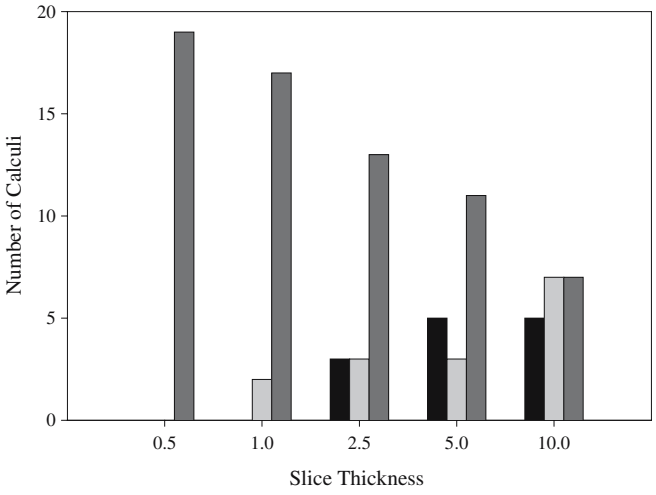

Fig. 2 Bar graph showing the effect of slice thickness on stone detection. The number of detectable calculi decreased as the section thickness increased ($P<0.001$). Scores: *darkly shaded bars*=2 (stone definitively present), *lightly shaded bars*=1 (stone possibly present), *black bars*=0 (stone not detectable)

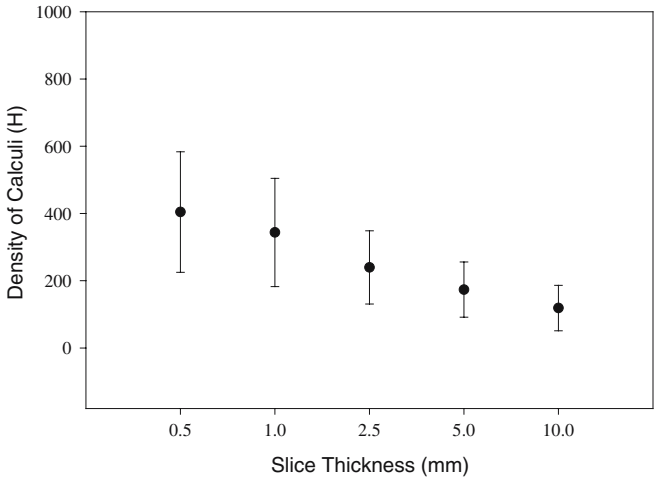

Fig. 4 Mean density of urinary calculi with standard deviation plotted against slice thickness. The measured attenuation value decreases as the slice thickness increases

detected on the thinner slices and progressively fewer as the slice thickness increased ($P<0.001$). Nineteen stones (100%) were detected on the 0.5-mm-thick slices, 17 (89%) on the 1.0-mm slices, 13 (68%) on the 2.5-mm slices, 11 (58%) on the 5.0-mm slices, and 7 (37%) on the 10.0-mm slices. All calculi with a diameter ≥2 mm were visible on the 0.5-mm, 1.0-mm, and 2.5-mm slices. One 3.1-mm cystine stone was not seen on the 5.0-mm slices. Three calculi of 2–2.9 mm (one of uric acid, one of cystine, and one of magnesium ammonium phosphate hexahydrate) and one calculus of 3–3.7 mm (cystine) were not seen on the 10.0-mm slices. However, the proportion of calculi of ≥2 mm detected at each slice thickness did not statistically differ ($P=0.109$). There was a significant correlation between the proportion of visible calculi <2 mm and the collimation ($P<0.001$). Of the nine calculi of 1–1.9 mm, nine (100%) were visible on the 0.5-mm slices, seven (78%) on the 1.0-mm images, three (33%) on the 2.5-mm images, and one (11%) on the 5.0-mm and 10.0-mm images.

The mean transverse diameter and density of the visible calculi decreased as the slice thickness increased (Figs. 3, 4). There was an inverse relationship between noise and slice thickness (Fig. 5). The relationship between noise and the square root of slice thickness was virtually linear ($r=0.988$; $P<0.001$).

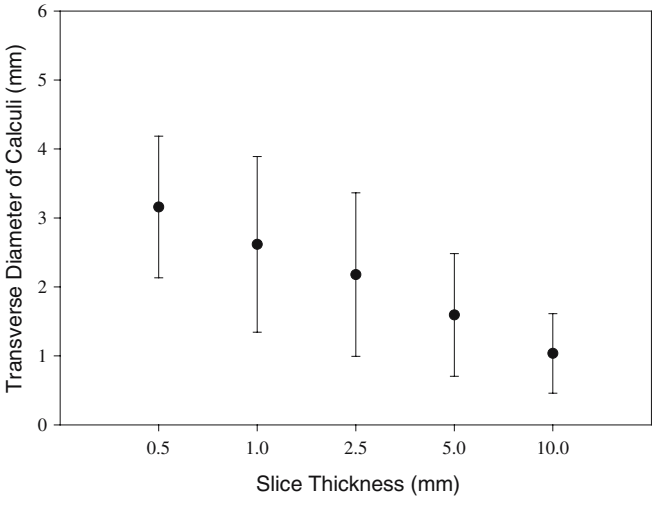

Fig. 3 Mean transverse diameter of urinary calculi with standard deviation plotted against slice thickness. The measured transverse diameter decreases as the slice thickness increases

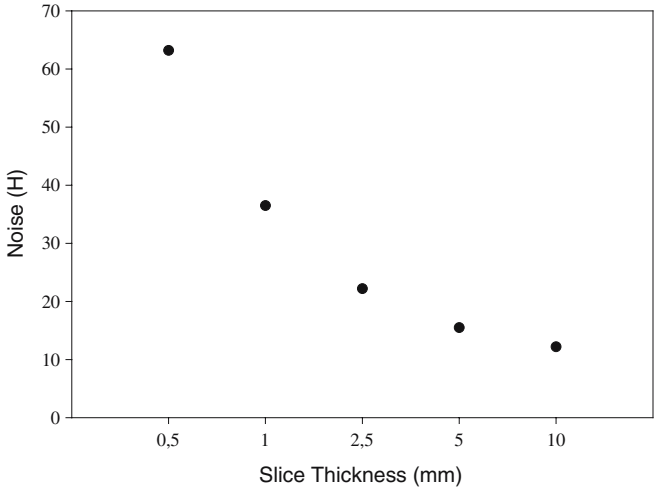

Fig. 5 Image noise plotted against slice thickness. Noise is inversely proportional to the square root of slice thickness ($P<0.001$)

Discussion

The results of this study show that the detection of small urinary calculi increases as the reconstructed slice thickness decreases. Decreasing the slice thickness has two opposing effects on the detection of small lesions. The detection can be improved by a decrease of partial volume effects, and it can be hampered by an increase in noise [23, 24]. In our study, better stone detection was obtained with thin slices at a constant dose, despite the increase of noise, because urinary calculi have a high contrast with the surrounding. High-contrast resolution is known to be independent of dose and noise within a certain range, whereas low-contrast resolution correlates with these two parameters [25, 26].

Our results are in accordance with the results of other high-contrast situations in the abdomen. Indeed, ex-vivo studies of CT colonography have shown that the detection of small polyps, which have a high contrast with the air in the colon, is greatly improved when the slice thickness is decreased, whereas the increase in dose has little effect [27, 28].

In contrast, the findings obtained in prior investigations of the utility of thin slices for the detection of low-contrast objects are controversial. A dual-detector CT system has shown that the use of 2.5-mm-thick slices yields greater conspicuity of small liver lesions than 5-mm images and improves lesion detection [29]. Conversely, more recent studies performed with four detector-row CT equipments have found little or no advantage in reducing slice thickness to less than 5 mm for the detection of liver metastases [30] or low-contrast structures in a phantom system [24]. In clinical practice, the reconstructed slice thickness in the abdomen usually remains 3–5 mm with 16-channel multidetector CT scanners [31].

In our study, the slice thickness affected not only the detection of urinary calculi, but also their characterization. We found that the average measured size and density of the calculi decreased when the slice thickness increased. The size of a urolithiasis is of critical importance in disease management [9, 10], and the perfromance of density measurements has been suggested for the prediction of the composition of urinary calculi [11–13]. With thick slices, errors in the determination of the size and composition of urinary calculi may place patients into an inappropriate treatment category. The effect of slice thickness on the attenuation of urinary calculi has also been previously observed by Saw et al. [32]. In addition, thin slices have recently been shown to be useful in the differentiation of urinary calculi from phleboliths [33].

Few attempts have been made to use slice thicknesses thinner than 5 mm to assess patients with renal colic since the introduction of CT for the detection of urinary calculi by Smith et al. in 1995 [17], although the possibility of overlooking small calculi has been recognized in the helical CT literature [5, 15–19]. After the advent of multidetector CT scanners, some authors still recommend the use of 5-mm-thick slices [20]. The proponents of this proposal use two arguments. The first one concerns the preservation of image quality. This argument is debatable as the detection of small high-contrast objects is improved when the slice thickness is decreased, as shown in our study, and the detection of low-contrast objects can be maintained by secondary thick reconstructions. The second argument concerns the clinical value of detecting small urinary calculi, as most of the calculi with a diameter of less than 4 mm will pass spontaneously. However, even calculi smaller than 2 mm may cause renal colic, have a delayed passage, and need intervention [8]. In the study of Coll et al., 13% of the ureteral calculi of 1 mm in diameter did not pass spontaneously and required intervention [10].

Despite the finding that even small calculi may cause symptoms, most of the clinical studies have been performed with 5-mm-thick slices. In contrast to these studies, we recommend the use of a thinner slice because this can improve the detection and the characterization of urinary calculi. We acknowledge that stone composition can also affect the detection rate. In our study, even larger calculi with low density (cystine, uric acid, and magnesium ammonium phosphate hexahydrate stones) were missed on the thick slices. However, stone composition did not bias our results, as stones of each chemical composition were included in each layer. In addition, density measurements were performed only on stones that were seen.

A limitation of our study is that the calculi were regularly spaced in the transverse plane. Therefore, the investigators were aware of the localization of the calculi in the phantom, and the false-positive rate could not be assessed. In addition, the study was conducted under nearly ideal conditions in a homogeneous non-anthropomorphic phantom, with fixed diameter and density. In clinical conditions, noise may become a more important problem, especially in the pelvis. However, secondary reconstructions of thicker slices can always be performed. With these thick reconstructed slices, the noise level is minimized and low-contrast information can be derived from the same raw data without multiple exposures [34]. This is particularly important when alternative diagnoses are sought in patients with suspected renal colic.

In conclusion, the results of the present study support the use of thin reconstructed slices to detect and characterize urinary calculi.

References

1. Smith RC, Verga M, McCarthy S, Rosenfield AT (1996) Diagnosis of acute flank pain: value of unenhanced helical CT. Am J Roentgenol 166:97–101
2. Abramson S, Walders N, Applegate KE, Gilkeson RC, Robbin MR (2000) Impact in the emergency department of unenhanced CT on diagnostic confidence and therapeutic efficacy in patients with suspected renal colic: a prospective survey. Am J Roentgenol 175:1689–1695
3. Pfister SA, Deckart A, Laschke S, Dellas S, Otto U, Buitrago C, Roth J, Wiesner W, Bongartz G, Gasser TC (2003) Unenhanced helical computed tomography vs intravenous urography in patients with acute flank pain: accuracy and economic impact in a randomized prospective trial. Eur Radiol 13:2513–2520
4. Olcott EW, Sommer FG, Napel S (1997) Accuracy of detection and measurement of renal calculi: in vitro comparison of three-dimensional spiral CT, radiography, and nephrotomography. Radiology 204:19–25
5. Levine JA, Neitlich J, Verga M, Dalrymple N, Smith RC (1997) Ureteral calculi in patients with flank pain: correlation of plain radiography with unenhanced CT. Radiology 204:27–31
6. Van Beers BE, Dechambre S, Hulcelle P, Materne R, Jamart J (2001) Value of multislice helical CT scans and maximum-intensity-projection images to improve detection of ureteral stones at abdominal radiography. Am J Roentgenol 177:1117–1121
7. Sheafor DH, Hertzberg BS, Freed KS, Carroll BA, Keogan MT, Paulson EK, DeLong DM, Nelson RC (2000) Nonenhanced helical CT and US in the emergency evaluation of patients with renal colic: prospective comparison. Radiology 217:792–797
8. Miller OF, Rineer SK, Reichard SR, Buckley RG, Donovan MS, Graham IR, Goff WB, Kane CJ (1998) Prospective comparison of unenhanced spiral computed tomography and intravenous urography in the evaluation of acute flank pain. Urology 52:982–987
9. Takahashi N, Kawashima A, Ernst RD, Boridy IC, Goldman SM, Benson GS, Sandler CM (1998) Ureterolithiasis: can clinical outcome be predicted with unenhanced helical CT? Radiology 208:97–102
10. Coll DM, Varanelli MJ, Smith RC (2002) Relationship of spontaneous passage of ureteral calculi to stone size and location as revealed by unenhanced helical CT. Am J Roentgenol 178:101–103
11. Saw KC, McAteer JA, Monga AG, Chua GT, Lingeman JE, Williams JC Jr (2000) Helical CT of urinary calculi: effect of stone composition, stone size, and scan collimation. Am J Roentgenol 175:329–332
12. Mostafavi MR, Ernst RD, Saltzman B (1998) Accurate determination of chemical composition of urinary calculi by spiral computerized tomography. J Urol 159:673–675
13. Bellin MF, Renard-Penna R, Conort P, Bissery A, Meric JB, Daudon M, Mallet A, Richard F, Grenier P (2004) Helical CT evaluation of the chemical composition of urinary tract calculi with a discriminant analysis of CT-attenuation values and density. Eur Radiol 14:2134–2140
14. Chen MY, Zagoria RJ, Saunders HS, Dyer RB (1999) Trends in the use of unenhanced helical CT for acute urinary colic. Am J Roentgenol 173: 1447–1450
15. Tublin ME, Murphy ME, Delong DM, Tessler FN, Kliewer MA (2002) Conspicuity of renal calculi at unenhanced CT: effects of calculus composition and size and CT technique. Radiology 225:91–96
16. Tamm EP, Silverman PM, Shuman WP (2003) Evaluation of the patient with flank pain and possible ureteral calculus. Radiology 228:319–329
17. Smith RC, Rosenfield AT, Choe KA, Essenmacher KR, Verga M, Glickman MG, Lange RC (1995) Acute flank pain: comparison of non-contrast-enhanced CT and intravenous urography. Radiology 194:789–794
18. Rimondini A, Pozzi Mucelli R, De Denaro M, Bregant P, Dalla Palma L (2001) Evaluation of image quality and dose in renal colic: comparison of different spiral-CT protocols. Eur Radiol 11:1140–1146
19. Tack D, Sourtzis S, Delpierre I, de Maertelaer V, Gevenois PA (2003) Low-dose unenhanced multidetector CT of patients with suspected renal colic. Am J Roentgenol 180:305–311
20. Katz DS, Venkataramanan N, Napel S, Sommer FG (2003) Can low-dose unenhanced multidetector CT be used for routine evaluation of suspected renal colic? Am J Roentgenol 180:313–315
21. Fuchs T, Kachelrieß M, Kalender WA (2000) Technical advances in multislice spiral CT. Eur J Radiol 36:69–73
22. Mahesh M, Scatarige JC, Cooper J, Fishman EK (2001) Dose and pitch relationship for a particular multislice CT scanner. Am J Roentgenol 177:1273–1275
23. Brooks RA, Di Chiro G (1976) Statistical limitations in X-ray reconstructive tomography. Med Phys 3:237–240
24. Verdun FR, Denys A, Valley JF, Schnyder P, Meuli RA (2002) Detection of low-contrast objects: experimental comparison of single- and multi-detector row CT with a phantom. Radiology 223:426–431
25. Scheck RJ, Coppenrath EM, Kellner MW, Lehmann KJ, Rock C, Rieger J, Rothmeier L, Schweden F, Bauml AA, Hahn K (1998) Radiation dose and image quality in spiral computed tomography: multicentre evaluation at six institutions. Br J Radiol 71:734–744
26. Shin HO, Falck CV, Galanski M (2004) Low-contrast detectability in volume rendering: a phantom study on multidetector-row spiral CT data. Eur Radiol 14:341–349
27. Wessling J, Fischbach R, Meier N, Allkemper T, Klusmeier J, Ludwig K, Heindel W (2003) CT colonography: protocol optimization with multi-detector row CT study in an anthropomorphic colon phantom. Radiology 228:753–759
28. Taylor SA, Halligan S, Bartram CI, Morgan PR, Talbot IC, Fry N, Saunders BP, Khosraviani K, Atkin W (2003) Multi-detector row CT colonography: effect of collimation, pitch, and orientation on polyp detection in a human colectomy specimen. Radiology 229:109–118
29. Weg N, Scheer MR, Gabor MP (1998) Liver lesions: improved detection with dual-detector-array CT and routine 2.5-mm thin collimation. Radiology 209:417–426
30. Haider MA, Amitai MM, Rappaport DC, O'Malley ME, Hanbidge AE, Redston M, Lockwood GA, Gallinger S (2002) Multi-detector row helical CT in preoperative assessment of small (≤1.5 cm) liver metastases: is thinner collimation better? Radiology 225:137–142
31. Saini S (2004) Multi-detector row CT: principles and practice for abdominal applications. Radiology 233:323–327
32. Saw KC, McAteer JA, Monga AG, Chua GT, Lingeman JE, Williams JC (2000) Helical CT of urinary calculi. Am J Roentgenol 175:329–332
33. Arac M, Celik H, Oner AY, Gultekin S, Gumus T, Kosar S (2005) Distinguishing pelvic phleboliths from distal ureteral calculi: thin-slice CT findings. Eur Radiol 15:65–70
34. Prokop M (2003) Multislice CT: technical principles and future trends. Eur Radiol 13:M3–M13